Report

Cell Reports

Cerebral electrometabolic coupling in disordered and normal states of consciousness

Graphical abstract

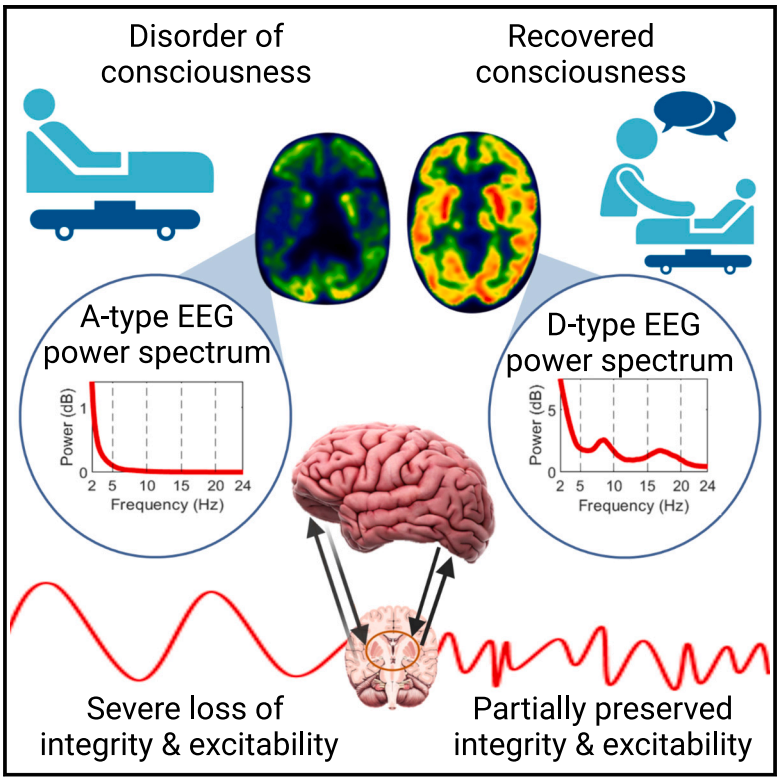

Authors

Jitka Annen, Gianluca Frasso, Glenn J.M. van der Lande, ..., Olivia Gosseries, Aurore Thibaut, Steven Laureys

Correspondence

jitka.annen@uliege.be

In brief

Patients with disorders of consciousness are characterized by reduced cerebral function as measured by glucose uptake and electrical activity. Annen et al. characterize the role of subcortical areas in sustaining cortical function and quantify electrometabolic coupling in healthy conscious and reduced conscious states after coma.

Highlights

- Biologically founded EEG spectral regimes are related to cortical glucose uptake
- Subcortical metabolism correlates with cortical α power, glucose uptake, and consciousness
- Cortical α is negatively and θ is positively related to cortical glucose uptake in controls
- Cortical electrometabolic coupling is inverted in patients with a severe brain injury

Annen et al., 2023, Cell Reports *42*, 112854
August 29, 2023
https://doi.org/10.1016/j.celrep.2023.112854

CellPress

Cell Reports

CellPress
OPEN ACCESS

Report

Cerebral electrometabolic coupling in disordered and normal states of consciousness

Jitka Annen,[1,2,9,*] Gianluca Frasso,[3] Glenn J.M. van der Lande,[1,2] Estelle A.C. Bonin,[1,2] Marie M. Vitello,[1,2] Rajanikant Panda,[1,2] Arianna Sala,[1,2] Carlo Cavaliere,[4] Federico Raimondo,[1,5] Mohamed Ali Bahri,[6] Nicholas D. Schiff,[7] Olivia Gosseries,[1,2] Aurore Thibaut,[1,2] and Steven Laureys[1,2,8]

[1]Coma Science Group, GIGA-Consciousness, University of Liège, Liège, Belgium
[2]Centre du Cerveau[2], University Hospital of Liège, Liège, Belgium
[3]Energy Efficiency, Samotics Bv, Leiden, the Netherlands
[4]IRCCS SYNLAB SDN of Naples, Naples, Italy
[5]Institute of Neuroscience and Medicine, Brain & Behaviour (INM-7), Research Centre Jülich, Jülich, Germany
[6]GIGA-Cyclotron Research Centre-In Vivo Imaging, University of Liège, Liège, Belgium
[7]BMRI, Weill Cornell Medicine, New York, NY, USA
[8]Joint International Research Unit on Consciousness, CERVO Brain Research Centre, University Laval, Quebec City, QC, Canada
[9]Lead contact
*Correspondence: jitka.annen@uliege.be
https://doi.org/10.1016/j.celrep.2023.112854

SUMMARY

We assess cerebral integrity with cortical and subcortical FDG-PET and cortical electroencephalography (EEG) within the mesocircuit model framework in patients with disorders of consciousness (DoCs). The mesocircuit hypothesis proposes that subcortical activation facilitates cortical function. We find that the metabolic balance of subcortical mesocircuit areas is informative for diagnosis and is associated with four EEG-based power spectral density patterns, cortical metabolism, and α power in healthy controls and patients with a DoC. Last, regional electrometabolic coupling at the cortical level can be identified in the θ and α ranges, showing positive and negative relations with glucose uptake, respectively. This relation is inverted in patients with a DoC, potentially related to altered orchestration of neural activity, and may underlie suboptimal excitability states in patients with a DoC. By understanding the neurobiological basis of the pathophysiology underlying DoCs, we foresee translational value for diagnosis and treatment of patients with a DoC.

INTRODUCTION

Cerebral integrity has been described to predict the behavior of patients with a disorder of consciousness (DoC).[1–3] Several neuroimaging techniques, including electroencephalography (EEG), e.g., Sitt et al.,[4] Engemann et al.,[5] and Lee et al.,[6] and fluorodeoxyglucose-positron emission tomography (FDG-PET) e.g., Thibaut et al.[3] and Stender et al.[7] can be used for the differential diagnosis of various classes of DoCs. However, some patients show preserved cerebral integrity at levels usually associated with conscious states[8] even in the absence of behavior, coining these erroneously considered unconscious patients as MCS* (non-behavioral minimally conscious state).[9] Simple spectral power measurements seem to be the most reliable EEG-based predictor for consciousness in patients with a DoC: specifically, lower levels of consciousness are characterized by increased δ power and, most importantly, by decreased α power.[4,5,10–12] The FDG-PET-based metabolic index (MIBH), as a proxy for metabolic activity in the best-preserved hemisphere,[13] validated by Hermann et al.,[14] can be used to identify levels of consciousness in patients with a DoC. Especially when extracted for the frontoparietal network (FPN), it can be used to detect covert consciousness.[8] Although a step toward the clinical translation of sensitive FDG-PET measures for the diagnosis of patients with a DoC is ongoing,[15] the lack of standardization of these quantitative assessment tools hampers clinical translation.

Furthermore, there is a pressing need to gain a better understanding of the neurobiological basis of DoCs.[16,17] In this regard, the theoretically based ABCD model[18] distinguishes four spectral regimes that are generated by specific lesions or levels of cerebral integrity and can be identified by evaluation of the power spectral density (PSD) of EEG.[19] An A-type PSD (i.e., dominant δ peak) appears after complete cortical deafferentation. B-type PSDs (i.e., dominant θ peak) reflect the pyramidal cells' intrinsic activity at 7 Hz functioning in isolation. The C-type PSD (i.e., both θ and β peaks) is generated by cortical activity in response to abnormal thalamic bursting during wakefulness under conditions of recovery of synaptic drive across a damaged thalamocortical radiation. The D-type PSD (i.e., dominant α and β peaks) marks a normal EEG with cortical activity and thalamic modulation. This classification predicts recovery of consciousness after acute brain injury.[19–22] The neurobiological basis of the ABCD model is grounded by the mesocircuit model, which proposes functional integrity within the

cortico-subcortical-cortical network to be crucial for consciousness.[23] Also in other neurological conditions such as temporal lobe and absence epilepsy, during an episode of transient loss of consciousness, thalamocortical projections are implicated by increasing synchrony to pathological levels, leading to loss of differentiation and complexity needed for consciousness.[24–27] In normal conditions, the striatum inhibits the internal globus pallidus, which disinhibits the thalamus. By this disinhibition, the thalamic projections excite the frontal, temporal, parietal, and occipital cortices that project back to subcortical nuclei, closing the functional loop. Any imbalance in this system causes reduced cortical excitation, predominantly in the FPN and the default mode network (DMN), which are directly anatomically connected[28] and centrally involved in consciousness.[29] A growing body of empirical evidence confirms that the mesocircuit mediates cortical activity and behavioral function.[28] For example, it was shown by Fridman et al. that glucose consumption within the subcortical parts of the network is positively associated with glucose metabolism in the FPN and with conscious behavior.[30] Indeed, using GABA-A-sensitive PET in a longitudinal study on patients with traumatic brain injury (TBI) showed that the excess of inhibition from the pallidum at follow up is associated with decreased anterior forebrain activity.[31] Precisely, the activity in the frontocortico-striatopallidal-thalamocortical loop, mediated by the anterior forebrain, might gradually recover function of the entire circuit and lead to (behavioral) recovery.[32] While holistic multimodal approaches assessing multiple aspects of the neurobiological processes underlying function are generally unexplored, they could inspire advancements for the prediction of outcome and treatment response.

By combining FDG-PET and resting-state, high-density EEG, we here study the neurobiological basis of cortical and subcortical dysfunction in a sample of patients with prolonged DoCs and patients who recovered from a DoC. Patients with DoCs include those with unresponsive wakefulness syndrome (UWS; also referred to as vegetative state [VS]),[33,34] where they are fully unconscious of themselves and the environment despite the presence of arousal. Patients in the minimally conscious state (MCS) present reproducible non-reflexive behaviors generated by conscious cortical activity.[34,35] By a combination of neuroimaging- and behavior-based diagnoses, patients who are covertly aware, also named e.g., MCS*[36] or patients with a cognitive motor dissociation, a subgroup of patients seemingly unconscious at the bedside yet presenting with neural activity associated with consciousness, can be defined. When patients, despite affected cognition due to widespread cortical lesions,[37,38] show the presence of functional communication or object use, they are considered emergent from the MCS (EMCS).[39] Patients with the locked-in syndrome (LIS) suffer from quadriplegia after brain injury yet usually can communicate using eye movements or assistive technologies.[40] In this retrospective study, we assess the cortical regimes of the ABCD model and relate them to levels of consciousness as diagnosed through behavior and glucose uptake (i.e., clinical examination and quantitative metrics). Given the pivotal role of subcortical areas, we assess their modulating role on cortical metabolic and electric activity. Last, we assess cortical electrometabolic coupling to investigate how glucose uptake relates to source-reconstructed EEG activity at the regional level. This multilevel and multimodal neuroimaging approach (1) assesses the clinical relevance of easy-to-interpret measures and (2) studies electrometabolic coupling in health and after brain injury to provide neurobiological insights in the generation of EEG rhythms.

RESULTS

Clinical and demographical characteristics are associated with electrophysiological integrity and glucose uptake of the FPN

11 healthy controls (HCs) and 22 patients did not differ in distribution of gender or age. Etiology and time since injury did not differ between the two patient groups (15 patients with a DoC and 7 patients recovered from a DoC). Please refer to the STAR Methods for descriptive statistics. The FDG-PET images provided a diagnosis of MCS for all patients with a DoC, deeming the patients in behavioral UWSs/VSs to be diagnosed as MCS*.[8] Table S1 presents subject-wise demographic, clinical, and neuroradiologic information.

The group presenting regime D consisted of 10 HCs, 2 patients with a DoC, and 5 patients recovered from a DoC (Figures 1A and 1B). Two patients with a DoC, 1 recovered patient, and one HC presented a C regime. The B regime was most prevalent (9 patients with a DoC and 1 recovered). Two patients with a DoC showed an A regime. The MIBH-FPN closely followed the ABCD spectral classification and decreased with more abnormal EEG regimes (D: median = 7.39, SD = 1.88; C: median = 5.98, SD = 1.70; B: median = 4.65, SD = 0.69; A: median = 3.76, SD = 1.12; Figure 1A) and behavioral diagnosis (DoC: 4.47 ± 1.30, recovered: 5.18 ± 1.38, $F(2,30) = 23.4$, $p < 0.0001$). Very similar group means were also observed for the whole-brain MIBH (D: median = 7.43, SD = 1.80; C: median = 5.73, SD = 1.83; B: median = 4.47, SD = 0.84; A: median = 3.76, SD = 1.05).

Subcortical glucose uptake balance is related to levels of consciousness, cortical glucose uptake, and cortical α power

The balance in glucose metabolism of the subcortical regions (i.e., thalamus and the ratio of globus pallidus/caudate uptake) was positively associated with the level of consciousness (left hemisphere: $F(2,30) = 28.7$, $p < 0.0001$; Fisher's least significant difference [LSD] DoC-control [$p < 0.0001$, 95% confidence interval (CI) (−8.14, −4.67)], Fisher's LSD recovered-control ($p < 0.001$, 95% CI [-6.45, −2.23]); Fisher's LSD DoC-recovered [$p < 0.05$, 95% CI (−4.07, −0.07)]; right hemisphere: $F(2,30) = 48.1$, $p < 0.0001$; Fisher's LSD DoC-control [$p < 0.0001$, 95% CI (−8.82, −5.78)]; Fisher's LSD recovered-control [$p < 0.0001$, 95% CI (−6.47, −2.77)]; Fisher's LSD DoC-recovered [$p < 0.01$, 95% CI (−4.43, −0.93)]; Figure 2A). Within the patients, the CRS-R index covaried with the subcortical mesocircuit metabolism in the left ($r = 0.46$, 95% CI [0.03, 0.74], $p < 0.05$) and right ($r = 0.56$, 95% CI [0.17, 0.79], $p < 0.01$) hemispheres. No relation between the subcortical metabolic balance and subcortical atrophy of the mesocircuit has been observed in either hemisphere.

A positive relation between the mesocircuit and cortical PET values was present in HCs for most cortical regions (Figure 2B). In patients who recovered consciousness, glucose metabolism

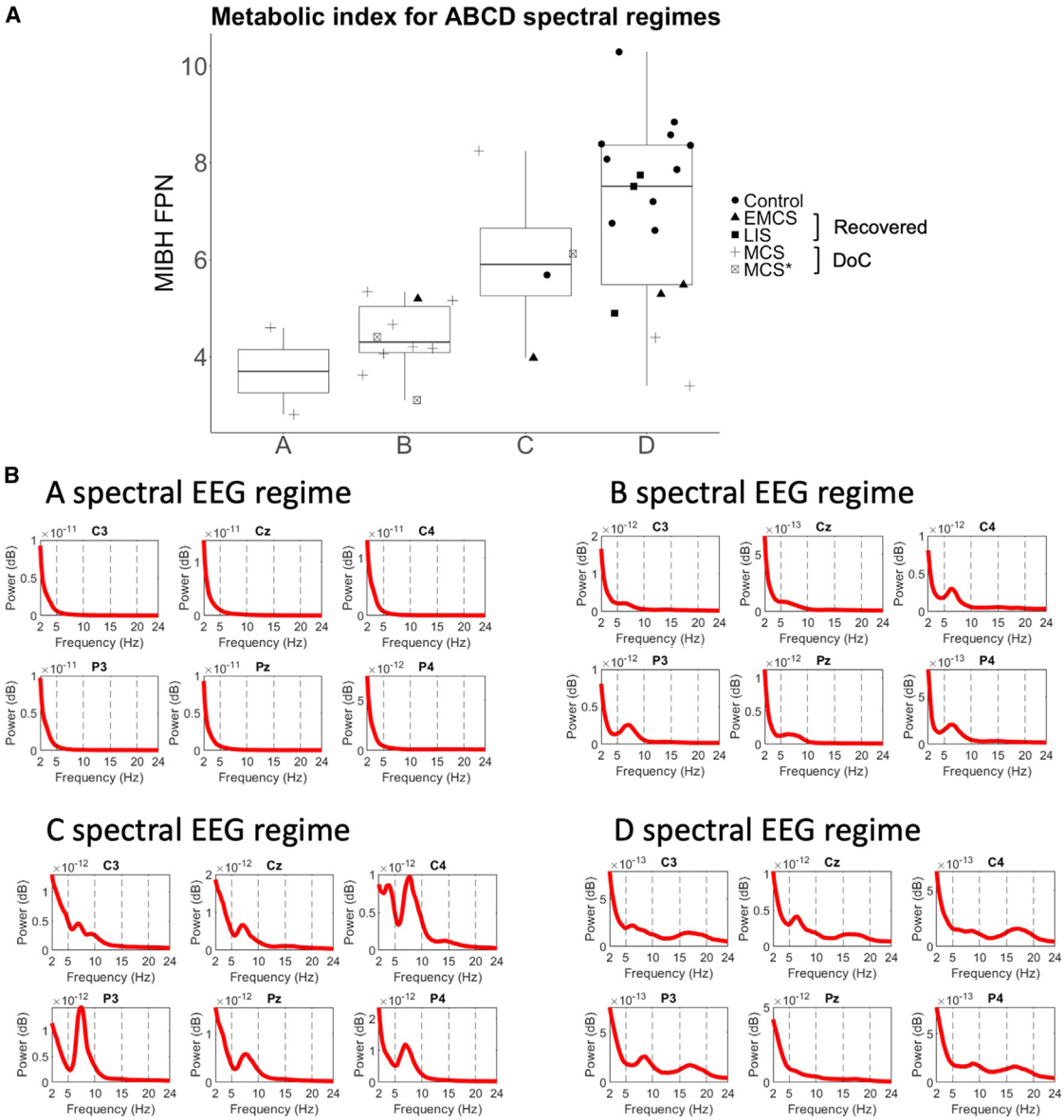

Figure 1. Diagnosis is associated with electrophysiological integrity and glucose uptake of the frontoparietal network

(A) Boxplot of the metabolic index in the frontoparietal network (MIBH-FPN), which increases alongside the normalization of the ABCD spectral regime (A = δ peak, B = θ peak, C = θ and β peaks, D = α and β peaks).

(B) Examples of the ABCD spectral regimes (Table S1 presents individual PSD overviews and MIBH-FPN values). HC, healthy control (n = 11); DoC, disorders of consciousness (n = 15); Recovered, recovered from a disorder of consciousness (n = 7).

in the inferior parietal, lateral-occipital, medial-orbito-frontal, and post-central regions was positively related to subcortical mesocircuit balance (Figure 2B). Patients with a DoC presented a positive relation between subcortical glucose uptake and metabolism in large parts of the FPN and the temporal cortex.

Glucose uptake balance within the subcortical areas of the mesocircuit was positively related to α power in several cortical areas in HCs and patients with a DoC (Figure 2B). In HCs, the association was the strongest in the fusiform gyrus, insula, pars orbitalis of the inferior frontal gyrus, and entorhinal, para-hippocampal, and inferior temporal cortices. In patients with a DoC, the relation was prominent in the anterior and posterior cingulate, superior frontal, and pre- and paracentral cortices. No association between the mesocircuit metabolism and cortical δ or θ activity was found.

Electrometabolic coupling at the cortical level: Cortical α and θ powers relate to cortical metabolism

A main effect of group on cerebral glucose uptake was evident, with lower values for patients with a DoC and patients recovered from a DoC than for healthy subjects (beta estimates, 95% confidence intervals and p values in Table 1). A negative main effect

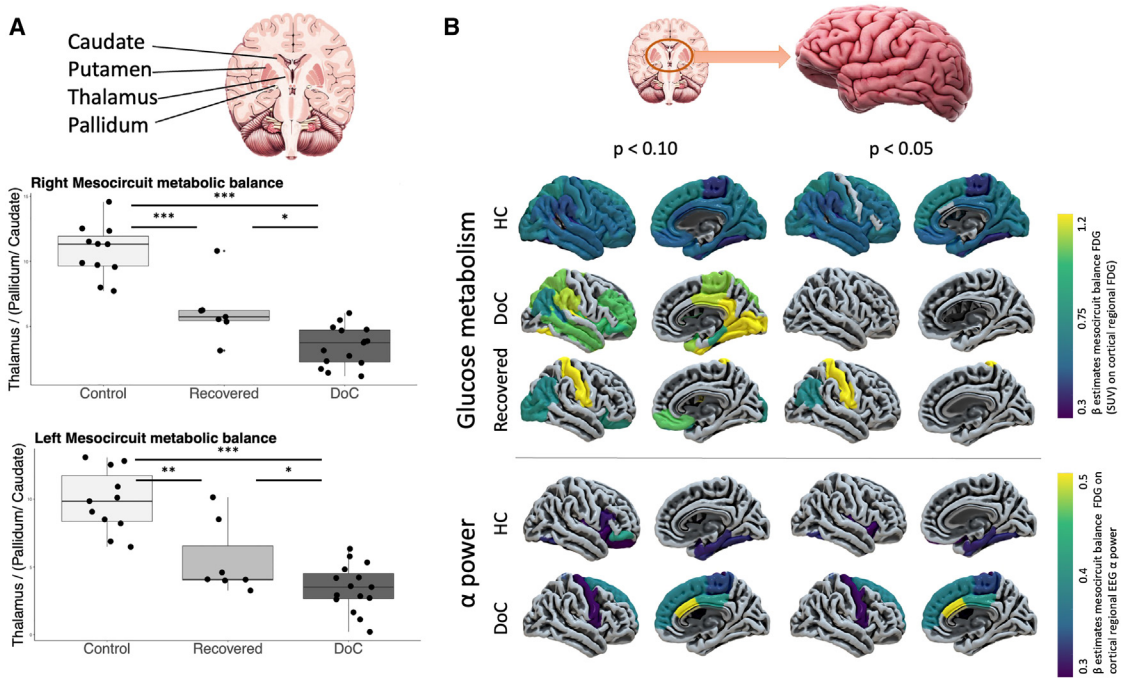

Figure 2. Subcortical glucose uptake balance is related to levels of consciousness, cortical glucose uptake, and cortical α power

(A) Boxplot of glucose uptake of subcortical structures of the mesocircuit differ between groups as assessed with ANOVA with post-hoc Fisher's LSD tests (***$p < 0.0001$, **$p < 0.001$, *$p < 0.05$).

(B) Beta estimates of linear regression models (presented for false discovery rate [FDR]-corrected $p < 0.05$ and $p < 0.1$) for the relation between subcortical metabolic balance and regional cortical function (i.e., with standardized uptake value [SUV] or normalized spectral power) per group. Note that in patients with a DoC, the results for the α power are equal for both significance levels and that the results for the glucose metabolism are not significant at $p < 0.05$. No results were obtained for the δ and θ bands. HC, healthy control (n = 11); DoC, disorders of consciousness (n = 15); Recovered, recovered from a disorder of consciousness (n = 7).

(i.e., considering the whole sample) of α power on glucose uptake at the cortical level was present. The relation between α power and glucose uptake was inverted in patients with a DoC and patients recovered from a DoC of our sample (linear effects in Figure 3). A positive main effect of θ power on glucose uptake was present. However, the effect was inverted in patients with a DoC compared with HCs.

DISCUSSION

Clinical and demographical characteristics are associated with electrophysiological integrity and glucose uptake of the FPN

The pathological EEG patterns of the ABCD spectral regimes were associated with low levels of consciousness (as in patients with acute brain injury, e.g., Forgacs et al.[19]) and glucose metabolism in the FPN and the whole brain. The concordance we have demonstrated between EEG and FDG-PET indicates a neurological basis for the EEG assessments. Yet, whether there is predictive value for the level of behavioral outcome in chronic patients with a DoC, as is the case for patients with acute TBI,[22] remains to be investigated. While more and increasingly complex metrics for consciousness are being developed continuously (e.g., for EEG, see Nilsen et al.[41]), the qualitative assessment of the four ABCD spectral regimes is biologically interpretable and can be translated to clinical application relatively easily. The ABCD spectral regime classification can be employed in patients with prolonged DoCs based on the PSD of six channels alone, without the need for quantitative analysis or assessment of connectivity or complexity. The approach aligns with international recommendations to supplement behavioral diagnoses of patients with a DoC with neuroimaging to reduce misdiagnosis.[42,43]

Subcortical glucose uptake balance is related to levels of consciousness and cortical glucose uptake

Our results indicate that the metabolic balance of the subcortical areas of the mesocircuit is related to the state of consciousness, with increasing metabolic activity in higher levels of consciousness, aligning with Fridman et al.[30] The relation holds when considering a fine-grained continuous scale of behavioral markers in patients with brain injuries, suggesting that the metabolic balance of the mesocircuit is a sensitive biomarker for conscious behavior. The absence of correlation between subcortical function and structure is surprising given the previously reported link between (subcortical) volume and behavior in patients with a DoC.[44,45]

Moreover, the glucose uptake balance of the subcortical areas was positively correlated with cortical glucose metabolism in HCs as expected in an intact mesocircuit that excites

Table 1. Beta estimates and 95% confidence intervals of linear mixed-effects model to assess electrometabolic coupling at the cortical level

	Estimated PVC-FDG (SUV)		
Predictors	Beta estimates	95% CI	p
Intercept	9.90	8.38–11.43	<0.001
Normalized α power	−24.34	−38.01–−10.66	<0.001
Recovered	−0.65	−2.92–1.62	0.573
DoC	−3.00	−5.01–−1.00	0.003
θ power	0.67	0.09–1.25	0.025
δ power	0.34	−0.32–1.01	0.309
α power * diagnosis recovered	26.68	10.44–42.93	0.001
α power * diagnosis DoC	35.98	18.01–53.95	<0.001
θ power * diagnosis recovered	−0.62	−1.27–0.03	0.062
θ power * diagnosis DoC	−0.83	−1.50–−0.15	0.017
δ power * diagnosis recovered	−0.17	−0.91–0.57	0.648
δ power * diagnosis DoC	−0.29	−0.97–0.38	0.398
Random effects			
σ2		4.69	
$\tau_{00\ Name}$		4.55	
ICC		0.49	
N_{Name}		33	
Observations		2,213	
Marginal R^2/conditional R^2		0.360/0.675	

DoC, disorder of consciousness (i.e., MCS* and MCS); Recovered, recovered from a disorder of consciousness (i.e., EMCS and LIS); SUV, standardized uptake value.

cortical function. In recovered patients and patients with a DoC, the effects were more localized. Although higher beta values were observed in patients, p values were lower, perhaps due to high inter-subject variability. In patients recovered from a DoC, the excitatory effects of the mesocircuit balance were strongest in post-central and occipital cortices. This might promote sensory processing by broadcasting of sensory input from the subcortex to the primary and higher-order somatosensory and visual areas, resonating with the belief that external awareness and successful interaction with an environment requires a functional balance between subcortical and cortical processing in low- and higher-order cortical areas.[46,47] The relation between subcortical and cortical glucose uptake in patients with a DoC was most prominent in the inferior-parietal and lateral-frontal cortices, which, together with the thalamus, form the FPN,[48] reported to be important to distinguish conscious states in DoCs.[29]

Electrometabolic coupling in the θ band

Cortical glucose uptake was positively related to θ power in the complete sample, like the positive relation between PET activity and θ power observed in HCs.[49] Although activity in the θ range is classically associated with drowsiness or sleepiness (e.g., Strijkstra et al.[50]), concordant with our observations, it might play a role in cognitive processes.[51] This might be mediated through DMN function,[52] the network often associated with conscious states.[53] In patients with a DoC, this effect is inverted, and higher θ power is associated with lower cortical metabolism. Indeed, widespread θ activity has been reported in DoCs, specifically in patients in the MCS.[11] Following the interpretation of the ABCD model, this θ peak could suggest that cortical neurons are not all lost but rather function in isolation due to partial thalamocortical deafferentation,[54] as the intrinsic oscillating frequency of pyramidal neurons is around 7 Hz.[55] That might be enough to recover simple signs of consciousness but not complex behaviors (i.e., as observed in EMCS, LIS, HCs) that require long-range interactions or recurrent activity hypothesized to be crucial for cognition. Local θ might thus be associated with consciousness and would call for a more fine-grained spatial assessment of θ power and the ABCD spectral regimes as in Curley et al.[22]

Besides the diagnostic utility of these results, the findings might have implications for the treatment of patients with a DoC. Although future electrometabolic coupling studies should help elucidate the mechanism and networks involved in recovery and help fine-tune treatment paradigms further, we speculate that by stimulating (midline) θ band electrical activity, glucose uptake and consciousness could potentially be increased. This might foster a (partial) normalization of the mesocircuit's activity as observed after pharmacological treatment (e.g., zolpidem[56]) or electrostimulation of the thalamus[57] or the vagus nerve.[58] Indeed, preliminary empirical support exists that θ power can facilitate the patients' brain to reach consciousness. Patients with a DoC responding to transcranial direct current stimulation treatment have higher resting-state θ power than patients not responsive to treatment,[59,60] and transcranial alternating current stimulation in the θ range does improve task performance in HCs.[61]

Electrometabolic coupling in the α band

Subcortical glucose uptake was positively related to α power in several cortical regions in HCs and patients with a DoC. Previous work shows that increased subcortical activity is associated with decreased α power in the cingulate cortex of HCs, as an index of cortical inactivity.[62] Our results, on the other hand, point toward a positive relation between subcortical glucose uptake and α power in the cingulate cortex of patients with a DoC. Given that α power in patients with a DoC is regarded as a positive predictor for consciousness, we speculate that the thalamus and the subcortical mesocircuit network more generally enable the generation of normalized α activity.

At the cortical level, glucose metabolism is, respectively, negatively and positively related to α power in HCs and patients with a DoC. Previous studies in HCs have found negative associations between α power and blood oxygenation level dependent (BOLD) as an indirect measure of glucose request during an awake state[63] and following sleep-induced loss of consciousness.[64] Tagliazucchi and

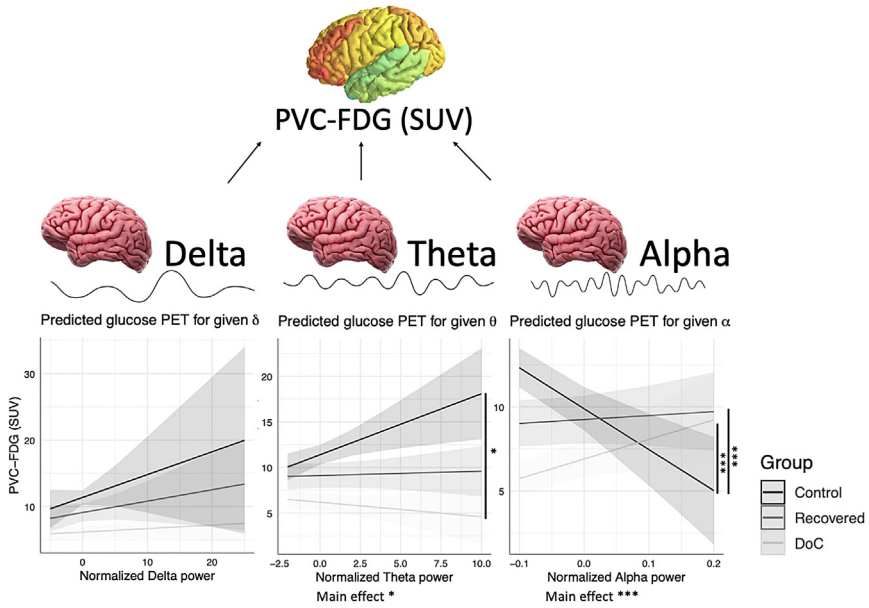

Figure 3. Electrometabolic coupling at the cortical level: θ and α relate to metabolism

Estimates of relations between cortical δ, θ, and α powers and cortical glucose uptake are presented per group (HCs n = 11, patients with a DoC n = 15, patients recovered from a DoC n = 7) as calculated with a linear mixed-effects model including 68 regional observations per subject, showing positive and negative main effects for θ and α power on glucose uptake, respectively. Interaction effects with diagnostic groups (plotted with a 95% confidence interval) show that the relation between θ power and glucose uptake is negative in the DoC sample, while α power is positively related to glucose uptake in patients with a DoC and those with recovered consciousness (***$p < 0.0001$, *$p < 0.05$).

colleagues interpreted their findings as the temporary functional weakening of local and long-range connectivity.[64] Others propose that α is cortically generated by short-range supragranular feedback loops, which in turn mediate activity in the thalamocortical system.[65] Also, the ABCD model proposes that the α peak (re)appears because of intact thalamocortical interactions and restoration of membrane depolarization in thalamic neurons sufficient to support tonic firing modes.[18] As such, it might modulate neural processing. Activity in the α range allows gating of information processing by inhibition (potentially of irrelevant information only)[66] and is, for example, suppressed when stimuli are perceived.[67] Moreover, power in the α range increases during eyes-closed rest and is observed at high amplitudes in patients in coma, both conditions during which neural processing is decreased.[68] Yet, activity in the α range is associated with higher levels of consciousness within the population of patients with a DoC at rest[4,5,12,69,70] and during tasks,[71] suggesting that it promotes neural processing. Based on the current observation of the potentially different roles of α in the orchestration of information processing in HCs and DoCs, we hypothesize that there is in an inverted U-shape relation between α power and optimal brain functioning such that the underlying neural activity is at an optimal excitability state (i.e., balance between excessive gating or suppression and unselective passage of information into the cortex), enabling thalamocortical interactions and cortical activity that support consciousness.

Although FDG-PET is considered the most accurate *in vivo* method for the (semi)quantification of cerebral glucose uptake in clinical settings,[72] it is impossible to distinguish excitatory and inhibitory activity using FDG-PET. Nevertheless, the bulk of cerebral glucose consumption can be attributed to neuronal activity given its high energy demand compared to astrocytes[73–75] and to excitatory neuronal activity in particular, stimulating aerobic glycolysis in astrocytes.[76] Neurophysiological computational models of brain dynamics as measured with EEG can model excitatory and inhibitory action between cortical and thalamic populations (e.g., Robinson et al.[77]) and would be best suited to address this in association with the mesocircuit model and ABCD spectral regimes.

Limitations of the study

The sample size is limited due to the challenging data acquisition and analyses. However, the employed statistics are conservative, and the results regarding cortical electrometabolic coupling consider many observations per subject. We were unable to assess differences in electrometabolic coupling between patients in the UWS/VS and MCS as did Coleman and colleagues,[78] who found electrometabolic coupling in patients in the MCS but not in the UWS/VS. Note that the patients in behaviorally UWSs/VSs included in the DoC sample are MCS* (based on FDG-PET), and as such, the observations of the study might represent patients in the MCS better than patients with a DoC. Moreover, the current study does not assess electrometabolic coupling in a longitudinal fashion, rendering it impossible to assess the stability of the observed effects over time and, moreover, to study if the (partial) normalization of activity in the whole brain is preceded by the anterior forebrain and the FPN as predicted by the mesocircuit model. Using dynamic causal modeling approaches would be a promising direction to address the causality of the relation between electrical and metabolic activity. Furthermore, the absence of any relation with δ activity, resulting from severe cortical deafferentation, is surprising, as this could have co-occurred with a lack of subcortical drive and loss of cortical metabolism, for which the thalamus is considered an important generator for δ.[79] Yet, only two patients with an A profile (i.e., δ peak only) were included. Last, accuracy source localization for the electrometabolic analysis,[80] especially in patients with brain injuries, is challenging. However, we only included patients with relatively intact cerebrums, and EEG source reconstruction has been performed successfully in patients with a DoC.[81] Given the concordance between the cortical electrometabolic coupling and ABCD classification at the scalp level, we

believe that source reconstruction did not introduce important biases.

STAR★METHODS

Detailed methods are provided in the online version of this paper and include the following:

- KEY RESOURCES TABLE
- RESOURCE AVAILABILITY
  - Lead contact
  - Materials availability
  - Data and code availability
- EXPERIMENTAL MODEL AND SUBJECT PARTICIPANT DETAILS
- METHOD DETAILS
  - Diagnosis of state of consciousness in patients with brain injury
  - Structural MRI
  - FDG-PET
  - High-density EEG
- QUANTIFICATION AND STATISTICAL ANALYSIS

SUPPLEMENTAL INFORMATION

Supplemental information can be found online at https://doi.org/10.1016/j.celrep.2023.112854.

ACKNOWLEDGMENTS

We are thankful to the patients and their families for their participation. The authors thank the entire staff from the Center du Cerveau[2], Radiodiagnostic and Nuclear Medicine departments, University Hospital of Liege. A.S. is postdoctoral fellow, O.G. and A.T. are research associates, and S.L. is research director at F.R.S.-FNRS. S.L. received funding from the European Union's Horizon 2020 Framework Programme for Research and Innovation under the Specific Grant Agreement No. 945539 (Human Brain Project SGA3). The study was further supported by the University and University Hospital of Liege and the European Commission.

AUTHOR CONTRIBUTIONS

Conceptualization, J.A. and S.L.; data acquisition, J.A., O.G., A.T., E.A.C.B., and M.M.V.; design, data curation, validation, and visualization, J.A. and G.F.; formal analysis, J.A., G.F., G.J.M.v.d.L., C.C., N.D.S., and R.P.; coding, J.A., G.F., F.R., M.A.B., and R.P.; writing – original draft, J.A.; writing – review & editing, J.A., G.F., A.T., O.G., A.S., G.J.M.v.d.L., C.C., E.A.C.B., M.M.V., N.D.S., and S.L.; funding acquisition, S.L., O.G., and A.T.; supervision, S.L.

DECLARATION OF INTERESTS

The authors declare no competing interests.

INCLUSION AND DIVERSITY

We support inclusive, diverse, and equitable conduct of research.

Received: October 19, 2022
Revised: June 2, 2023
Accepted: July 8, 2023
Published: July 26, 2023

REFERENCES

1. Annen, J., Frasso, G., Crone, J.S., Heine, L., Perri, C.D., Martial, C., Cassol, H., Demertzi, A., Naccache, L., Laureys, S., et al. (2018). Regional brain volumetry and brain function in severely brain-injured patients. Annals *Accepted a*, pp. 1–28.
2. Aubinet, C., Murphy, L., Bahri, M.A., Larroque, S.K., Cassol, H., Annen, J., Carrière, M., Wannez, S., Thibaut, A., Laureys, S., and Gosseries, O. (2018). Brain, behavior, and cognitive interplay in disorders of consciousness: A multiple case study. Front. Neurol. *9*, 665. https://doi.org/10.3389/fneur.2018.00665.
3. Thibaut, A., Bruno, M.A., Chatelle, C., Gosseries, O., Vanhaudenhuyse, A., Demertzi, A., Schnakers, C., Thonnard, M., Charland-Verville, V., Bernard, C., et al. (2012). Metabolic activity in external and internal awareness networks in severely brain-damaged patients. J. Rehabil. Med. *44*, 487–494. https://doi.org/10.2340/16501977-0940.
4. Sitt, J.D., King, J.-R., El Karoui, I., Rohaut, B., Faugeras, F., Gramfort, A., Cohen, L., Sigman, M., Dehaene, S., and Naccache, L. (2014). Large scale screening of neural signatures of consciousness in patients in a vegetative or minimally conscious state. Brain *137*, 2258–2270. https://doi.org/10.1093/brain/awu141.
5. Engemann, D.A., Raimondo, F., King, J.-R., Rohaut, B., Louppe, G., Faugeras, F., Annen, J., Cassol, H., Gosseries, O., Fernandez-Slezak, D., et al. (2018). Robust EEG-based cross-site and cross-protocol classification of states of consciousness. Brain *141*, 3179–3192. https://doi.org/10.1093/brain/awy251.
6. Lee, M., Sanz, L.R.D., Barra, A., Wolff, A., Nieminen, J.O., Boly, M., Rosanova, M., Casarotto, S., Bodart, O., Annen, J., et al. (2022). Quantifying arousal and awareness in altered states of consciousness using interpretable deep learning. Nat. Commun. *13*, 1064–1114. https://doi.org/10.1038/s41467-022-28451-0.
7. Stender, J., Gosseries, O., Bruno, M.-A., Charland-Verville, V., Vanhaudenhuyse, A., Demertzi, A., Chatelle, C., Thonnard, M., Thibaut, A., Heine, L., et al. (2014). Diagnostic precision of PET imaging and functional MRI in disorders of consciousness: a clinical validation study. Lancet *384*, 514–522. https://doi.org/10.1016/S0140-6736(14)60042-8.
8. Thibaut, A., Panda, R., Annen, J., Sanz, L.R.D., Naccache, L., Martial, C., Chatelle, C., Aubinet, C., Bonin, E.A.C., Barra, A., et al. (2021). Preservation of Brain Activity in Unresponsive Patients Identifies MCS Star. Ann. Neurol. *90*, 89–100. https://doi.org/10.1002/ANA.26095.
9. Gosseries, O., Di, H., Laureys, S., and Boly, M. (2014). Measuring Consciousness in Severely Damaged Brains. Annu. Rev. Neurosci. *37*, 457–478. https://doi.org/10.1146/annurev-neuro-062012-170339.
10. Chennu, S., Finoia, P., Kamau, E., Allanson, J., Williams, G.B., Monti, M.M., Noreika, V., Arnatkeviciute, A., Canales-Johnson, A., Olivares, F., et al. (2014). Spectral Signatures of Reorganised Brain Networks in Disorders of Consciousness. PLoS Comput. Biol. *10*, e1003887. https://doi.org/10.1371/journal.pcbi.1003887.
11. Schiff, N.D., Nauvel, T., and Victor, J.D. (2014). Large-scale brain dynamics in disorders of consciousness. Curr. Opin. Neurobiol. *25*, 7–14. https://doi.org/10.1016/j.conb.2013.10.007.
12. Chennu, S., Annen, J., Wannez, S., Thibaut, A., Chatelle, C., Cassol, H., Martens, G., Schnakers, C., Gosseries, O., Menon, D., and Laureys, S. (2017). Brain networks predict metabolism, diagnosis and prognosis at the bedside in disorders of consciousness. Brain *140*, 2120–2132. https://doi.org/10.1093/brain/awx163.
13. Stender, J., Mortensen, K.N., Thibaut, A., Darkner, S., Laureys, S., Gjedde, A., and Kupers, R. (2016). The Minimal Energetic Requirement of Sustained Awareness after Brain Injury. Curr. Biol. *26*, 1494–1499. https://doi.org/10.1016/j.cub.2016.04.024.
14. Hermann, B., Stender, J., Habert, M.O., Kas, A., Denis-Valente, M., Raimondo, F., Pérez, P., Rohaut, B., Sitt, J.D., and Naccache, L. (2021). Multimodal FDG-PET and EEG assessment improves diagnosis and

prognostication of disorders of consciousness. Neuroimage. Clin. *30*, 102601. https://doi.org/10.1016/J.NICL.2021.102601.

15. Sala, A., Schindele, A., Beliy, N., Bernard, C., Panda, R., Phillips, C., Mohamed, A.B., Laureys, S., Gosseries, O., Thibaut, A., et al. (2022). An automated FDG-PET pipeline for the analysis of glucose brain metabolism in disorders of consciousness. In Journal of Cerebral Blood Flow and Metabolism : Official Journal of the International Society of Cerebral Blood Flow and Metabolism, pp. 108–273, NLM (Medline). https://doi.org/10.1177/0271678X221096357.
16. Goldfine, A.M., and Schiff, N.D. (2011). Consciousness: Its Neurobiology and the Major Classes of Impairment. Neurol. Clin. *29*, 723–737. https://doi.org/10.1016/J.NCL.2011.08.001.
17. Luppi, A.I., Cain, J., Spindler, L.R.B., Górska, U.J., Toker, D., Hudson, A.E., Brown, E.N., Diringer, M.N., Stevens, R.D., Massimini, M., et al. (2021). Mechanisms Underlying Disorders of Consciousness: Bridging Gaps to Move Toward an Integrated Translational Science. Neurocritical Care *35*, 37–54. https://doi.org/10.1007/S12028-021-01281-6.
18. Schiff, N.D. (2016). Mesocircuit mechanisms underlying recovery of consciousness following severe brain injuries: Model and predictions. In Brain Function and Responsiveness in Disorders of Consciousness (Springer International Publishing), pp. 195–204. https://doi.org/10.1007/978-3-319-21425-2_15.
19. Forgacs, P.B., Frey, H.P., Velazquez, A., Thompson, S., Brodie, D., Moitra, V., Rabani, L., Park, S., Agarwal, S., Falo, M.C., et al. (2017). Dynamic regimes of neocortical activity linked to corticothalamic integrity correlate with outcomes in acute anoxic brain injury after cardiac arrest. Ann. Clin. Transl. Neurol. *4*, 119–129. https://doi.org/10.1002/ACN3.385.
20. Eliseyev, A., Der-Nigoghossian, C.A., Alkhachroum, A., Rubinos, C., Kromm, J.A., Mathews, E., Bauerschmidt, A., Doyle, K., Velasquez, A., Egbebike, J.A., et al. (2020). EEG to detect early recovery of consciousness in amantadine-treated acute brain injury patients. J. Neurol. Neurosurg. Psychiatry *91*, 675–676. https://doi.org/10.1136/JNNP-2019-322645.
21. Frohlich, J., Crone, J.S., Johnson, M.A., Lutkenhoff, E.S., Spivak, N.M., Dell'Italia, J., Hipp, J.F., Shrestha, V., Ruiz Tejeda, J.E., Real, C., et al. (2022). Neural oscillations track recovery of consciousness in acute traumatic brain injury patients. Hum. Brain Mapp. *43*, 1804–1820. https://doi.org/10.1002/HBM.25725.
22. Curley, W.H., Bodien, Y.G., Zhou, D.W., Conte, M.M., Foulkes, A.S., Giacino, J.T., Victor, J.D., Schiff, N.D., and Edlow, B.L. (2022). Electrophysiological correlates of thalamocortical function in acute severe traumatic brain injury. Cortex *152*, 136–152. https://doi.org/10.1016/J.CORTEX.2022.04.007.
23. Schiff, N.D. (2010). Recovery of consciousness after brain injury: a mesocircuit hypothesis. Trends Neurosci. *33*, 1–9. https://doi.org/10.1016/j.tins.2009.11.002.
24. Arthuis, M., Valton, L., Régis, J., Chauvel, P., Wendling, F., Naccache, L., Bernard, C., and Bartolomei, F. (2009). Impaired consciousness during temporal lobe seizures is related to increased long-distance cortical–subcortical synchronization. Brain *132*, 2091–2101. https://doi.org/10.1093/BRAIN/AWP086.
25. Bartolomei, F. (2012). Coherent neural activity and brain synchronization during seizure-induced loss of consciousness. Arch. Ital. Biol. *150*, 164–171. https://doi.org/10.4449/AIB.V150I2.1252.
26. Bartolomei, F., McGonigal, A., and Naccache, L. (2014). Alteration of consciousness in focal epilepsy: The global workspace alteration theory. Epilepsy Behav. *30*, 17–23. https://doi.org/10.1016/J.YEBEH.2013.09.012.
27. El Youssef, N., Jegou, A., Makhalova, J., Naccache, L., Bénar, C., and Bartolomei, F. (2022). Consciousness alteration in focal epilepsy is related to loss of signal complexity and information processing. Sci. Rep. *12*, 22276. https://doi.org/10.1038/s41598-022-25861-4.
28. Schiff, N.D. (2022). Mesocircuit mechanisms in the diagnosis and treatment of disorders of consciousness. Presse Med. *52*, 104161. https://doi.org/10.1016/j.lpm.2022.104161.
29. Heine, L., Soddu, A., Gómez, F., Vanhaudenhuyse, A., Tshibanda, L., Thonnard, M., Charland-Verville, V., Kirsch, M., Laureys, S., and Demertzi, A. (2012). Resting state networks and consciousness: alterations of multiple resting state network connectivity in physiological, pharmacological, and pathological consciousness States. Front. Psychol. *3*, 1–12. https://doi.org/10.3389/fpsyg.2012.00295.
30. Fridman, E. a, Beattie, B.J., Broft, A., Laureys, S., and Schiff, N.D. (2014). Regional cerebral metabolic patterns demonstrate the role of anterior forebrain mesocircuit dysfunction in the severely injured brain. Proc. Natl. Acad. Sci. USA *111*, 6473–6478. https://doi.org/10.1073/pnas.1320969111.
31. Kang, Y., Jamison, K., Jaywant, A., Dams-O'Connor, K., Kim, N., Karakatsanis, N.A., Butler, T., Schiff, N.D., Kuceyeski, A., and Shah, S.A. (2022). Longitudinal alterations in gamma-aminobutyric acid (GABAA) receptor availability over ~ 1 year following traumatic brain injury. Brain Commun. *4*, fcac159. https://doi.org/10.1093/BRAINCOMMS/FCAC159.
32. Schiff, N.D. (2010). Recovery of consciousness after brain injury: a mesocircuit hypothesis. Trends Neurosci. *33*, 1–9. https://doi.org/10.1016/j.tins.2009.11.002.Recovery.
33. Giacino, J.T., Kalmar, K., and Whyte, J. (2004). The JFK Coma Recovery Scale-Revised: Measurement characteristics and diagnostic utility. Arch. Phys. Med. Rehabil. *85*, 2020–2029. https://doi.org/10.1016/j.apmr.2004.02.033.
34. Giacino, J.T., and Kalmar, K. (1997). The vegetative and minimally conscious states: A comparison of clinical features and functional outcome. J. Head Trauma Rehabil. *12*, 36–51.
35. Rosenbaum, A.M., and Giacino, J.T. (2015). Clinical Management of the Minimally Conscious State, 1st ed. (Elsevier B.V.). https://doi.org/10.1016/B978-0-444-52892-6.00025-8.
36. Schnakers, C., Bauer, C., Formisano, R., Noé, E., Llorens, R., Lejeune, N., Farisco, M., Teixeira, L., Morrissey, A.M., De Marco, S., et al. (2022). What names for covert awareness? A systematic review. Front. Hum. Neurosci. *16*, 971315. https://doi.org/10.3389/FNHUM.2022.971315.
37. Schnakers, C., Majerus, S., Goldman, S., Boly, M., van Eeckhout, P., Gay, S., Pellas, F., Bartsch, V., Peigneux, P., Moonen, G., and Laureys, S. (2008). Cognitive function in the locked-in syndrome. J. Neurol. *255*, 323–330. https://doi.org/10.1007/s00415-008-0544-0.
38. Bodien, Y.G., Martens, G., Ostrow, J., Sheau, K., and Giacino, J.T. (2020). Cognitive impairment, clinical symptoms and functional disability in patients emerging from the minimally conscious state. NeuroRehabilitation *46*, 65–74. https://doi.org/10.3233/NRE-192860.
39. Giacino, J.T., Fins, J.J., Laureys, S., and Schiff, N.D. (2014). Disorders of consciousness after acquired brain injury: the state of the science. Nat. Rev. Neurol. *10*, 99–114. https://doi.org/10.1038/nrneurol.2013.279.
40. Smith, E., and Delargy, M. (2005). Locked-in syndrome. Britisch Medical Journal *330*, 406–409.
41. Nilsen, A.S., Juel, B., Thürer, B., and Storm, J.F. Proposed EEG Measures of Consciousness: A Systematic, Comparative Review. 10.31234/OSF.IO/SJM4A.
42. Kondziella, D., Bender, A., Diserens, K., van Erp, W., Estraneo, A., Formisano, R., Laureys, S., Naccache, L., Ozturk, S., Rohaut, B., et al. (2020). European Academy of Neurology guideline on the diagnosis of coma and other disorders of consciousness. Eur. J. Neurol. *27*, 741–756. https://doi.org/10.1111/ENE.14151.
43. Giacino, J.T., Katz, D.I., Schiff, N.D., Whyte, J., Ashman, E.J., Ashwal, S., Barbano, R., Hammond, F.M., Laureys, S., Ling, G.S.F., et al. (2018). Practice Guideline Update Recommendations Summary: Disorders of Consciousness: Report of the Guideline Development, Dissemination, and Implementation Subcommittee of the American Academy of Neurology; the American Congress of Rehabilitation Medicine; and the National Institute on Disability, Independent Living, and Rehabilitation Research. Arch. Phys. Med. Rehabil. *99*, 1699–1709. https://doi.org/10.1016/j.apmr.2018.07.001.

44. Lutkenhoff, E.S., Chiang, J., Tshibanda, L., Kamau, E., Kirsch, M., Pickard, J.D., Laureys, S., Owen, A.M., and Monti, M.M. (2015). Thalamic and extrathalamic mechanisms of consciousness after severe brain injury. Ann. Neurol. *78*, 68–76. https://doi.org/10.1002/ana.24423.

45. Annen, J., Frasso, G., Crone, J.S., Heine, L., Di Perri, C., Martial, C., Cassol, H., Demertzi, A., Naccache, L., and Laureys, S.; Coma Science Group Collaborators (2018). Regional brain volumetry and brain function in severely brain-injured patients. Ann. Neurol. *83*, 842–853. https://doi.org/10.1002/ana.25214.

46. Vanhaudenhuyse, A., Demertzi, A., Schabus, M., Noirhomme, Q., Bredart, S., Boly, M., Phillips, C., Soddu, A., Luxen, A., Moonen, G., and Laureys, S. (2011). Two distinct neuronal networks mediate the awareness of environment and of self. J. Cognit. Neurosci. *23*, 570–578. https://doi.org/10.1162/jocn.2010.21488.

47. Mashour, G.A., Roelfsema, P., Changeux, J.P., and Dehaene, S. (2020). Conscious Processing and the Global Neuronal Workspace Hypothesis. Neuron *105*, 776–798. https://doi.org/10.1016/J.NEURON.2020.01.026.

48. Raichle, M.E., MacLeod, A.M., Snyder, A.Z., Powers, W.J., Gusnard, D.a., and Shulman, G.L. (2001). A default mode of brain function. Proc. Natl. Acad. Sci. USA *98*, 676–682. https://doi.org/10.1073/pnas.98.2.676.

49. Pizzagalli, D.A., Oakes, T.R., and Davidson, R.J. (2003). Coupling of theta activity and glucose metabolism in the human rostral anterior cingulate cortex: An EEG/PET study of normal and depressed subjects. Psychophysiology *40*, 939–949. https://doi.org/10.1111/1469-8986.00112.

50. Strijkstra, A.M., Beersma, D.G.M., Drayer, B., Halbesma, N., and Daan, S. (2003). Subjective sleepiness correlates negatively with global alpha (8-12 Hz) and positively with central frontal theta (4-8 Hz) frequencies in the human resting awake electroencephalogram. Neurosci. Lett. *340*, 17–20. https://doi.org/10.1016/S0304-3940(03)00033-8.

51. Kahana, M.J., Seelig, D., and Madsen, J.R. (2001). Theta returns. Curr. Opin. Neurobiol. *11*, 739–744. https://doi.org/10.1016/S0959-4388(01)00278-1.

52. Florin, E., and Baillet, S. (2015). The brain's resting-state activity is shaped by synchronized cross-frequency coupling of neural oscillations. Neuroimage *111*, 26–35. https://doi.org/10.1016/j.neuroimage.2015.01.054.

53. Demertzi, A., Soddu, A., and Laureys, S. (2013). Consciousness supporting networks. Curr. Opin. Neurobiol. *23*, 239–244. https://doi.org/10.1016/j.conb.2012.12.003.

54. Llinás, R.R., Ribary, U., Jeanmonod, D., Kronberg, E., and Mitra, P.P. (1999). Thalamocortical dysrhythmia: A neurological and neuropsychiatric syndrome characterized by magnetoencephalography. Proc. Natl. Acad. Sci. USA *96*, 15222–15227.

55. Silva, L.R., Amitai, Y., and Connors, B.W. (1991). Intrinsic oscillations of neocortex generated by layer 5 pyramidal neurons. Science *251*, 432–435. https://doi.org/10.1126/science.1824881.

56. Thonnard, M., Gosseries, O., Demertzi, A., Lugo, Z., Vanhaudenhuyse, A., Bruno, M.-A., Chatelle, C., Thibaut, A., Charland, V., Laureys, S., et al. (2012). An open label prospective study on the effect of zolpidem in chronic disorders of consciousness. Brain Inj. *26*, 668–669.

57. Schiff, N.D., Giacino, J.T., Kalmar, K., Victor, J.D., Baker, K., Gerber, M., Fritz, B., Eisenberg, B., O'Connor, J., O'Connor, J., et al. (2007). Behavioral improvements with thalamic stimulation after severe traumatic brain injury. Nature *448*, 600–603. https://doi.org/10.1038/nature06041.

58. Briand, M.M., Gosseries, O., Staumont, B., Laureys, S., and Thibaut, A. (2020). Transcutaneous Auricular Vagal Nerve Stimulation and Disorders of Consciousness: A Hypothesis for Mechanisms of Action. Front. Neurol. *11*, 933. https://doi.org/10.3389/FNEUR.2020.00933.

59. Thibaut, A., Chennu, S., Chatelle, C., Martens, G., Annen, J., Cassol, H., and Laureys, S. (2018). Theta network centrality correlates with tDCS response in disorders of consciousness. Brain Stimul. *11*, 1407–1409. https://doi.org/10.1016/j.brs.2018.09.002.

60. Hermann, B., Raimondo, F., Hirsch, L., Huang, Y., Denis-Valente, M., Pérez, P., Engemann, D., Faugeras, F., Weiss, N., Demeret, S., et al. (2020). Combined behavioral and electrophysiological evidence for a direct cortical effect of prefrontal tDCS on disorders of consciousness. Sci. Rep. *10*, 4323. https://doi.org/10.1038/S41598-020-61180-2.

61. Jaušovec, N., Jaušovec, K., and Pahor, A. (2014). The influence of theta transcranial alternating current stimulation (tACS) on working memory storage and processing functions. Acta Psychol. *146*, 1–6. https://doi.org/10.1016/j.actpsy.2013.11.011.

62. Goldman, R.I., Stern, J.M., Engel, J., Jr., and Cohen, M.S. (2012). Simultaneous EEG and fMRI of the alpha rhythm. Neuroreport *13*, 1–5, Simultaneous. https://doi.org/10.1097/01.wnr.0000047685.08940.d0.

63. de Munck, J.C., Gonçalves, S.I., Huijboom, L., Kuijer, J.P.A., Pouwels, P.J.W., Heethaar, R.M., and Lopes da Silva, F.H. (2007). The hemodynamic response of the alpha rhythm: An EEG/fMRI study. Neuroimage *35*, 1142–1151. https://doi.org/10.1016/j.neuroimage.2007.01.022.

64. Tagliazucchi, E., von Wegner, F., Morzelewski, A., Brodbeck, V., and Laufs, H. (2012). Dynamic BOLD functional connectivity in humans and its electrophysiological correlates. Front. Hum. Neurosci. *6*, 339–422. https://doi.org/10.3389/fnhum.2012.00339.

65. Halgren, M., Ulbert, I., Bastuji, H., Fabó, D., Erőss, L., Rey, M., Devinsky, O., Doyle, W.K., Mak-McCully, R., Halgren, E., et al. (2019). The generation and propagation of the human alpha rhythm. Proc. Natl. Acad. Sci. USA *116*, 23772–23782. https://doi.org/10.1073/PNAS.1913092116.

66. Jensen, O., and Mazaheri, A. (2010). Shaping Functional Architecture by Oscillatory Alpha Activity: Gating by Inhibition. Front. Hum. Neurosci. *4*, 186–188. https://doi.org/10.3389/fnhum.2010.00186.

67. Gaillard, R., Dehaene, S., Adam, C., Clémenceau, S., Hasboun, D., Baulac, M., Cohen, L., and Naccache, L. (2009). Converging Intracranial Markers of Conscious Access. PLoS Biol. *7*, e1000061. https://doi.org/10.1371/JOURNAL.PBIO.1000061.

68. Berkhoff, M., Donati, F., and Bassetti, C. (2000). Postanoxic alpha (theta) coma: A reappraisal of its prognostic significance. Clin. Neurophysiol. *111*, 297–304. https://doi.org/10.1016/S1388-2457(99)00246-1.

69. Fingelkurts, A.A., Fingelkurts, A.A., Bagnato, S., Boccagni, C., and Galardi, G. (2012). EEG oscillatory states as neuro-phenomenology of consciousness as revealed from patients in vegetative and minimally conscious states. Conscious. Cognit. *21*, 149–169. https://doi.org/10.1016/j.concog.2011.10.004.

70. Lehembre, R., Marie-Aurélie, B., Vanhaudenhuyse, A., Chatelle, C., Cologan, V., Leclercq, Y., Soddu, A., Macq, B., Laureys, S., and Noirhomme, Q. (2012). Resting-state EEG study of comatose patients: a connectivity and frequency analysis to find differences between vegetative and minimally conscious states. Funct. Neurol. *27*, 41–47.

71. Goldfine, A.M., Victor, J.D., Conte, M.M., Bardin, J.C., and Schiff, N.D. (2011). Determination of awareness in patients with severe brain injury using EEG power spectral analysis. Clin. Neurophysiol. *122*, 2157–2168. https://doi.org/10.1016/j.clinph.2011.03.022.

72. Guedj, E., Varrone, A., Boellaard, R., Albert, N.L., Barthel, H., van Berckel, B., Brendel, M., Cecchin, D., Ekmekcioglu, O., Garibotto, V., et al. (2021). EANM procedure guidelines for brain PET imaging using [18F]FDG, version 3. Eur. J. Nucl. Med. Mol. Imag. *49*, 632–651. https://doi.org/10.1007/S00259-021-05603-W.

73. Mergenthaler, P., Lindauer, U., Dienel, G.A., and Meisel, A. (2013). Sugar for the brain : the role of glucose in physiological and pathological brain function. Trends Neurosci. *36*, 587–597. https://doi.org/10.1016/j.tins.2013.07.001.

74. Chatton, J.Y., Pellerin, L., and Magistretti, P.J. (2003). GABA uptake into astrocytes is not associated with significant metabolic cost: Implications for brain imaging of inhibitory transmission. Proc. Natl. Acad. Sci. USA *100*, 12456–12461. https://doi.org/10.1073/PNAS.2132096100.

75. Howarth, C., Gleeson, P., and Attwell, D. (2012). Updated energy budgets for neural computation in the neocortex and cerebellum. J. Cereb. Blood Flow Metab. *32*, 1222–1232. https://doi.org/10.1038/jcbfm.2012.35.

76. Stoessl, A.J. (2017). Glucose utilization: still in the synapse. Nat. Neurosci. *20*, 382–384. https://doi.org/10.1038/nn.4513.

77. Robinson, P.A., Rennie, C.J., Rowe, D.L., O'Connor, S.C., Wright, J.J., Gordon, E., and Whitehouse, R.W. (2003). Neurophysical Modeling of Brain Dynamics. Neuropsychopharmacology *28*, S74–S79. https://doi.org/10.1038/sj.npp.1300143.

78. Coleman, M.R., Menon, D.K., Fryer, T.D., and Pickard, J.D. (2005). Neurometabolic coupling in the vegetative and minimally conscious states: preliminary findings. J. Neurol. Neurosurg. Psychiatry *76*, 432–434. https://doi.org/10.1136/jnnp.2004.045930.

79. Neske, G.T. (2015). The slow oscillation in cortical and thalamic networks: Mechanisms and functions. Front. Neural Circ. *9*, 88. https://doi.org/10.3389/FNCIR.2015.00088/BIBTEX.

80. Wendel, K., Väisänen, O., Malmivuo, J., Gencer, N.G., Vanrumste, B., Durka, P., Magjarević, R., Supek, S., Pascu, M.L., Fontenelle, H., and Grave de Peralta Menendez, R. (2009). EEG/MEG Source Imaging : Methods , Challenges , and Open Issues. Comput. Intell. Neurosci. *2009*, 656092. https://doi.org/10.1155/2009/656092.

81. Rizkallah, J., Annen, J., Modolo, J., Gosseries, O., Benquet, P., Mortaheb, S., Amoud, H., Cassol, H., Mheich, A., Thibaut, A., et al. (2019). Decreased integration of EEG source-space networks in disorders of consciousness. Neuroimage. Clin. *23*, 101841. https://doi.org/10.1016/j.nicl.2019.101841.

82. Annen, J., Heine, L., Ziegler, E., Frasso, G., Bahri, M., Perri, C. di, Stender, J., Martial, C., Wannez, S., D, K., et al. (2016). Function – Structure Connectivity in Patients with Severe Brain Injury as Measured by MRI-DWI and FDG-PET. Hum Brain Mapp *00*. https://doi.org/10.1002/hbm.23269.

83. Annen, J., Filippini, M.M., Bonin, E., Cassol, H., Aubinet, C., Carrière, M., Gosseries, O., Thibaut, A., Barra, A., Wolff, A., et al. (2019). Diagnostic accuracy of the CRS-R index in patients with disorders of consciousness. Brain Inj. *33*, 1409–1412. https://doi.org/10.1080/02699052.2019.1644376.

84. Tadel, F., Baillet, S., Mosher, J.C., Pantazis, D., and Leahy, R.M. (2011). Brainstorm: A user-friendly application for MEG/EEG analysis. Comput. Intell. Neurosci. *2011*, 879716. https://doi.org/10.1155/2011/879716.

85. Oostenveld, R., Fries, P., Maris, E., Schoffelen, and FieldTrip, J-.M. (2011). Open Source Software for Advanced Analysis of MEG, EEG, and Invasive Electrophysiological Data. Computational Intelligence and Neuroscience *2011*, 156869. https://doi.org/10.1155/2011/156869.

86. Wannez, S., Heine, L., Thonnard, M., Gosseries, O., Laureys, S., and Collaborators, C.S.G. (2018). The repetition of behavioral assessments in diagnosis of disorders of consciousness. Ann. Neurol. *1–20*.

87. Fischl, B., Sereno, M.I., Tootell, R.B., and Dale, a M. (1999). High-resolution intersubject averaging and a coordinate system for the cortical surface. Hum. Brain Mapp. *8*, 272–284. https://doi.org/10.1002/(SICI)1097-0193.

88. Desikan, R.S., Ségonne, F., Fischl, B., Quinn, B.T., Dickerson, B.C., Blacker, D., Buckner, R.L., Dale, A.M., Maguire, R.P., Hyman, B.T., et al. (2006). An automated labeling system for subdividing the human cerebral cortex on MRI scans into gyral based regions of interest. Neuroimage *31*, 968–980. https://doi.org/10.1016/j.neuroimage.2006.01.021.

89. Fischl, B., Salat, D.H., Busa, E., Albert, M., Dieterich, M., Haselgrove, C., van der Kouwe, A., Killiany, R., Kennedy, D., Klaveness, S., et al. (2002). Neurotechnique Whole Brain Segmentation: Automated Labeling of Neuroanatomical Structures in the Human Brain. Neuron *33*, 341–355.

90. Hansen, T.I., Brezova, V., Eikenes, L., Håberg, A., and Vangberg, T.R. (2015). How Does the Accuracy of Intracranial Volume Measurements Affect Normalized Brain Volumes? Sample Size Estimates Based on 966 Subjects from the HUNT MRI Cohort. AJNR Am J Neuroradiol *M*. AJNR. Am. J. Neuroradiol. *36*, 1450–1456. https://doi.org/10.3174/ajnr.A4299.

91. Evans, W.A. (1942). An encephalographic ratio for estimating ventricular enlargement and cerebral atrophy. Arch. Neurol. Psychiatr. *47*, 931.

92. Müller-Gärtner, H.W., Links, J.M., Prince, J.L., Bryan, R.N., McVeigh, E., Leal, J.P., Davatzikos, C., and Frost, J.J. (1992). Measurement of radiotracer concentration in brain gray matter using positron emission tomography: MR-based correction for partial volume effects. J. Cerebr. Blood Flow Metabol. *12*, 571–583.

93. Rousset, O., Rahmim, A., Alavi, A., and Zaidi, H. (2007). Partial Volume Correction Strategies in PET. Pet. Clin. *2*, 235–249. https://doi.org/10.1016/j.cpet.2007.10.005.

94. Quarantelli, M., Berkouk, K., Prinster, A., Landeau, B., Svarer, C., Balkay, L., Alfano, B., Brunetti, A., Baron, J.-C., and Salvatore, M. (2004). Integrated software for the analysis of brain PET/SPECT studies with partial-volume-effect correction. J. Nucl. Med. *45*, 192–201.

95. Svarer, C., Madsen, K., Hasselbalch, S.G., Pinborg, L.H., Haugbøl, S., Frøkjaer, V.G., Holm, S., Paulson, O.B., and Knudsen, G.M. (2005). MR-based automatic delineation of volumes of interest in human brain PET images using probability maps. Neuroimage *24*, 969–979. https://doi.org/10.1016/j.neuroimage.2004.10.017.

96. Sokoloff, L., Reivich, M., Kennedy, C., Des Rosiers, M.H., Patlak, C.S., Pettigrew, K.D., Sakurada, O., and Shinohara, M. (1977). The [14C]deoxyglucose method for the measurement of local cerebral glucose utilization: theory, procedure, and normal values in the conscious and anesthetized albino rat. J. Neurochem. *28*, 897–916. https://doi.org/10.1111/J.1471-4159.1977.TB10649.X.

97. Annen, J., Heine, L., Ziegler, E., Frasso, G., Bahri, M., Di Perri, C., Stender, J., Martial, C., Wannez, S., D'ostilio, K., et al. (2016). Function–structure connectivity in patients with severe brain injury as measured by MRI-DWI and FDG-PET. Hum. Brain Mapp. *37*, 3707–3720. https://doi.org/10.1002/hbm.23269.

98. R Core team (2012). R: A Language and Environment for Statistical Computing (R Foundation for Statistical Computing). http://www.r-project.org/.

STAR★METHODS

KEY RESOURCES TABLE

REAGENT or RESOURCE	SOURCE	IDENTIFIER
Deposited data		
FDG-PET	University of Liege	https://doi.org/10.25493/7TXP-WCF
Software and algorithms		
Structure function	Annen et al.[82]	https://doi.org/10.5281/zenodo.8082598
CRS-R index	Annen et al.[83]	https://doi.org/10.5281/zenodo.8082587
MATLAB 2017a	MathWorks	https://www.mathworks.com
Brainstorm	Tadel et al.[84]	https://neuroimage.usc.edu/brainstorm
Freesurfer	Athinoula A. Martinos Center for Biomedical Imaging	https://surfer.nmr.mgh.harvard.edu
Fieldtrip	Oostenveld et al.[85]	https://www.fieldtriptoolbox.org/

RESOURCE AVAILABILITY

Lead contact

Further information and requests for resources and data should be directed to and will be fulfilled by the lead contact, Jitka Annen (jitka.annen@uliege.be).

Materials availability

This study did not generate new material.

Data and code availability

- Part of the PET data (https://doi.org/10.25493/7TXP-WCF) is available in the Human Brain Project initiative's EBRAINS knowledge graph. EEG data can be obtained after request. Please note that T1 MRI data is not shared publicly due to anonymization challenges.
- Several freely available toolboxes are used for data analysis (see method details section below). In-house code for the regional FDG-PET uptake extraction is available (https://doi.org/10.5281/zenodo.8082598). Code to calculate the CRS-R index is available (https://doi.org/10.5281/zenodo.8082587).
- Any additional information required to reanalyze the data reported in this work paper is available from the lead contact upon request.

EXPERIMENTAL MODEL AND SUBJECT PARTICIPANT DETAILS

88 patients were hospitalized (between April 2011 and February 2017) in the University Hospital of Liège for a one-week assessment of consciousness using at least 5 CRS-R assessments, high-density EEG, (T1-weighted) MRI, and FDG-PET. Alongside the patients, 15 healthy control subjects (HC) were submitted to the same evaluation protocol (i.e., minus the CRS-R). Due to the scientific rather than clinical objectives of this study, strict inclusion criteria regarding data quality (i.e., good EEG and FDG-PET data, not more than severe brain injury in >2/3 of one hemisphere) were maintained leading to a high number of excluded patients (75%) and HC (26%). Patients were excluded from this study when presented with pre-insult neurological illness, non-compatibility with either MRI or PET, or when less than 18 years of age. Two HC were excluded because of bad quality EEG, and for two the FOV of the T1 image did not include the whole skull rendering the image not usable for source reconstruction.

The final sample consisted of 15 patients with a DoC (i.e., MCS and MCS*), 7 patients recovered from a DoC (i.e., EMCS and LIS, post-comatose patients who regained functional communication or object use), and 11 healthy control subjects (HC). The HC (5 female, mean age = 42.3 ± 14.3) and patients (5 female, mean age = 34.5 ± 16.1) did not differ in distribution of gender ($C^2(1) = 2.14$, $p = 0.35$) or age ($t(18.1) = 1.36$, $p = 0.19$). Etiology (DoC 9, recovered 4 with traumatic brain injury, $C^2(1) = 0.02$, $p = 0.89$) and time since injury (DoC 3.1 ± 3.0, recovered 7.9 ± 8.8 years, (5.5) = 1.28, p = 0.25) did not differ between the two patient groups (15 DoC and 7 recovered). The study was approved by the Ethical committee of the University of Liège. Patients' legal guardians and HC gave written informed consent for participation in the study, in accordance with the declaration of Helsinki.

METHOD DETAILS

Diagnosis of state of consciousness in patients with brain injury

Diagnosis was based on neuroimaging assessment with FDG-PET[7] and the best out of at least five CRS-R evaluations, to reduce misdiagnosis.[86] When the behavioral and neuroimaging diagnosis gave conflicting results, patients for whom the behavioral diagnosis was UWS and neuroimaging suggested MCS were diagnosed as MCS*. From the best CRS-R evaluation, the CRS-R index was calculated. This index is a linear transformation of the CRS-R subscores, and unlike the CRS-R total score, can diagnose patients in the UWS/VS and MCS on a single dimension.[83] The CRS-R index ranges from 0 to 100, with a cut-off for consciousness at 8.315. To calculate the score, it first distinguishes between behavioral items that rely on reflexes (i.e., subcortical structures) and consciousness (i.e., cortical function) for every subscale (auditory, visual, motor and oromotor function, communication and arousal) of the CRS-R. By combining the reflex and consciousness scores a unified score from the conversion matric is obtained, to which the arousal score is added. Code to calculate the CRS-R index can be found at https://doi.org/10.5281/zenodo.8082587. The diagnosis based on behavior was verified with FDG-PET, as described in more detail below.

Structural MRI

MRI data was acquired using a 3 Tesla scanner (Siemens Trio, Siemens, Germany). Structural MRI data were obtained with T1-weighted 3D gradient echo images using 120 slices, repetition time of 2,300 ms, echo time of 2.47 ms, voxel size of 1 × 1 × 1.2 mm^3, a flip angle of 98° and a data matrix of 256 x 256 mm^3. The T1-weighted MRI's of each subject were manually reoriented to the orientation of the MNI 152 1mm^3 template. Freesurfer (v 5.3.0[87]) was used to automatically label GM/WM and CSF, as well as every region of interest (ROI) of the cerebrum using the Desikan-Kiliany atlas[88] as in.[45] The subcortical segmentation was performed by the default pipeline of Freesurfer based on probabilistic information of the location of subcortical structures, using the Aseg atlas.[89] The segmented volumes of the bilateral thalamus, pallidum and caudate have been extracted and normalized for total intracranial volume.[90] The quality of the segmentation and parcellation was visually evaluated and patients for whom problems occurred in any of these steps were excluded from the study (about 1/3 of the patients). A certified neuroradiologist (CC) assessed the T1-weighted MRI of every patient to assess the most prominent damage and Evans' index (see Table S1). The Evans' index is a measure of ventricular volume and is a rough biomarker of hydrocephalus (normal values <0.30).[91]

FDG-PET

The FDG PET scan was performed on a Gemini TF PET-CT scanner (Philips, USA), about 30 min after intravenous bolus injection of 150–300 MBq of FDG, as described in.[82] A low-dose CT scan was acquired for attenuation correction, followed by a 12-min PET emission scan. All PET images were reconstructed using the iterative list mode time-of-flight LOR-OSEM algorithm, and corrections for attenuation, dead-time, random events, and scatter were applied. With this acquisition and reconstruction settings, images had 2mm^3 isotropic voxels in a 256 × 256 × 89 voxel matrix (sample can be found at https://doi.org/10.25493/7TXP-WCF). FDG-PET images were manually reoriented toward the T1-weighted image using Statistical Parametric Mapping toolbox (www.fil.ion.ucl.ac.uk/spm) in order to ease later automated registration tasks. Neuroimaging based diagnosis of DoC is an important supplementary step to improve clinical diagnosis.[42,43] For this purpose, we here used a well-established visual classification protocol relying on FPN metabolism preservation.[7] Preserved metabolism in this network is observed in patients with an FDG-PET diagnosis of MCS, while hypometabolism of this network is associated to an FDG-PET diagnosis of UWS/VS. A semi-quantitative assessment of whole brain metabolism to diagnose patients with a DoC was provided with the MIBH of the best-preserved hemisphere[13] and the FPN[8] (AAL atlas regions used to define the network: 2, 7–10, 38–40, 42–48, 50, 55–58, 86–88, 90–96).

For the multimodal EEG, MRI and FDG-PET analysis, FDG-PET images underwent partial volume effect (PVE) correction using the Müller-Gärtner-Rousset method[92,93] and a point spread function of 8mm as implemented in PVE-lab (version 2.2[94,95]). To perform the PVE correction, a rigid-body transformation was applied to the GM, WM, and CSF segmentations to bring them into the space of the PET image. Following PVE correction the PET image was transformed into T1 space and the mean SUV value was extracted within each ROI using in-house software (https://doi.org/10.5281/zenodo.8082598). The assessment is semi-quantitative because glucose uptake was used as proxy for glucose metabolism as measured with the standardized uptake value (SUV) or metabolic index which is highly correlated with the gold standard Cerebral Metabolic Rate for glucose as based on.[96] This process yielded the mean partial volume effect-correct glucose uptake of 68 gray matter regions (Desikan-Kiliany atlas) per subject as in.[97]

High-density EEG

The EEG data has been acquired using the Hydro-Cel GSN electrode net (Electric Geodesics, EGI) with 256 sponge electrodes soaked in saline solution to obtain high density coverage of the scalp. The EGI amplifier sampling rate was set to 250 or 500Hz (the latter was down-sampled to 250Hz afterward for consistency). EEG data were collected, with hardware reference to Cz, in resting state conditions and simultaneous with FDG uptake for the PET scan. Data collection was performed in a dark and quiet room, and the experimenter, present throughout the recording, ensured the subject was awake and with eyes open. EEG acquisition started about 10 min before injection until 20–30 min just before the start of the PET acquisition. This approach allows for the simultaneous acquisition of the EEG and FDG-PET data, the latter being a static scan representing the total neural activity that occurred during the FDG uptake period.

High-density resting state EEG data was preprocessed using in-house software based on MNE-python (https://www.martinos.org/mne/stable/index.html). Data cleaning included the following steps: continuous EEG was down-sampled to 250Hz, filtered (6th order Butterworth high pass filter at 0.5Hz and a 8th order butter-worth low pass filter at 100Hz with notches at 50 and 100Hz), epoched in 2.2s segments, bad channels were rejected on the basis of visual inspection of the raw timeseries, and bad segments were selected in PCA space (i.e., the timeseries were transformed into 20 PCA components). Full ICA was performed on the cleaned data and components corresponding to non-neural activity were removed from the data. Last, bad channels were interpolated, data was referenced to average reference and the first 5 clean minutes of data was extracted, as the impedances are best at the beginning of the recording.

Power spectrum distribution (PSD) plots for all subjects were for the visual classification of ABCD spectral regimes of cortical activity that could be linked to corticothalamic integrity.[18,19] Frequency analysis was performed using fieldtrip V. 20220617 (https://www.fieldtriptoolbox.org/).[85] A Slepian taper sequence using 3 tapers was used to extract power at frequencies from 1 Hz to 30 Hz in steps of 0.25 Hz. The data was zero padded to the next power of two and output was smoothed on a 1 Hz scale. Power was plotted between 2 Hz and 24 Hz for channels Cz, C3, C4, Pz, P3, P4 and the average activity of all channels for the whole-brain PSD as in.[19] Visual inspection of the PSD was performed by two independent assessors (JA, GJML) blinded to the diagnosis. The classification of the four different classes (i.e., ABCD; A dominant δ peak, B appearance of θ peak, C presence of θ and β peaks, D presence of α and β peaks) was agreed upon in case of disagreement between assessors, and validated by a third independent assessor (NDS).

For the purpose of the multimodal electrometabolic coupling analysis including EEG, T1 and FDG-PET analysis the following steps were performed. Clean EEG data was filtered in separate frequency bands (i.e., δ 1-4Hz, θ 4-7Hz, α 7-12Hz) for source reconstruction. Source reconstruction was performed using every subject own cortical meshes as obtained from Freesurfer. The MRI and EEG were co-registered though anatomical landmarks (nasion and left and right tragus) as implemented in Brainstorm,[84] a MATLAB toolbox (version 2017a). The lead-field matrix was calculated using openMEEG (BEM model, with 1922 vertices per mesh) with the dSPM method (obtaining Z-scores for source reconstructed activation values), restricted to cortical sources. Per frequency band, the diagonal noise covariance was calculated, and per ROI (i.e., 68 cortical ROIs) the mean and standard deviation of the power in each frequency band was extracted and subsequently normalized.

QUANTIFICATION AND STATISTICAL ANALYSIS

Statistics were performed in R,[98] considering all subjects from all groups. Gender differences between patients and HC, and etiology (TBI or non TBI) differences between patient groups (recovered and DoC) were assessed with a chi-square test. T-tests assessed differences in the distribution of age between patients and HC, and days since injury onset for the patient groups. Descriptive statistics for the MIBH-FPN and ABCD classifications were provided in the results section and Figure 1.

The mesocircuit model was tested by evaluating the equilibrium of the subcortical network's activity as the ratio of glucose uptake in the Thalamus (measured with SUV) divided by the ratio of globus pallidus/caudate uptakes (i.e., subcortical mesocircuit balance). This balance reflects the inhibiting input from the caudate to the globus pallidus and the disinhibiting input from the globus pallidus to the thalamus to scale the excitatory input from the thalamus to the cortex, as hypothesized by the anterior forebrain mesocircuit model for recovery of consciousness. We tested the hypothesis of an increase in this ratio for higher consciousness levels using an ANOVA with post-hoc comparisons (The Fisher's LSD Least Significant Different, considered significant at $p < 0.05$, Figure 2A). Pearson correlation coefficients were calculated for the mesocircuit metabolism (for the left and right hemisphere) and CRS-R index (considering patients only, considered significant at $p < 0.025$, see results). To quantify subcortical atrophy each structure's volume was scaled by the maximum volume in healthy volunteers. Then, for both hemispheres the atrophy in each subcortical network was calculated as the average atrophy of the three structures (i.e., thalamus, caudate and pallidum). The atrophy measure was correlated to the glucose uptake balance in the subcortical parts of the mesocircuit using a spearman correlation (see results).

The relation between cortical function (dependent variables, as measured by EEG - in α, θ and δ bands - or FDG-PET) and subcortical mesocircuit balance (independent variable) was modeled in each group (i.e., HC, recovered and DoC). Linear regression models were fit to correlate the subcortical metabolic balance with cortical glucose uptake (SUV), normalized δ, θ and α power in the 34 cortical ROIs (i.e., parcellated using the Desikan-Killiany atlas[88] and averaged between left and right hemispheres). The coefficients' p values were FDR-corrected, and the beta estimates for $p < 0.05$ and $p < 0.1$ are displayed on a cortical template brain using the Surface toolbox (Figure 2B). We present results at $p < 0.1$ as well for two reasons. First, the beta values for the patient groups were higher than for the HC, suggesting a stronger effect in patients or a ceiling effect in HC, despite the lower p values (perhaps due to more variability in the latter). Second, we would like to avoid false negative results, which especially in modest sample sizes, are likely to occur with multiple comparison corrections.

We used a linear mixed effects model (with a random intercept for subject) to test for regional relations between spectral power and glucose uptake on the whole-brain level. Fixed effects were included for group (i.e., healthy subjects, patients with a DoC and patients recovered from a DoC), the normalized power in every frequency band (i.e., δ, θ, α), and their respective interaction (Figure 3). This analysis considers the electrometabolic relation per subject across all regions (i.e., 68 observations) and does not account for the spatial dependence amongst regions. Predictors are considered significant at $p < 0.05$ (Table 1 for beta estimates and 95% confidence intervals).